Organometallics **2005,** *24,* 1161−1172

Selective Metallacyclization and Crystallographic Characterization of Structurally Related Platina-annulenes

Charles A. Johnson, II and Michael M. Haley*

Department of Chemistry and Materials Science Institute, University of Oregon, Eugene, Oregon 97403-1253

Elisabeth Rather, Fusen Han, and Timothy J. R. Weakley

X-ray Crystallography Laboratory, Department of Chemistry, University of Oregon, Eugene, Oregon 97403-1253

Received November 20, 2004

The synthesis and characterization of seven platina-annulenes and their dehydrobenzoannulene (DBA) analogues are reported. Assembly of these macrocycles is accomplished via Sn transmetalation or amine-mediated oxidative addition with stoichiometric $PtCl_2(PR_3)_2$, containing different phosphine ligands, and CuI. In contrast to previously reported DBA cyclization methodology, incorporation of a doubly σ-bonded Pt complex into the annulene backbone resulted in selective metallacyclization dependent on competing factors of ligand identity, $PtCl_2(PR_3)_2$ isomer, and reaction conditions. Sn transmetalation conditions provided the most selective metallacyclization control and prevented $PtCl_2(PR_3)_2$ isomerization during cyclization.

Introduction

Highly conjugated, organometallic "rigid-rod" oligomers and polymers continue to be investigated for potential use as advanced materials with desirable electronic and optical properties.[1] In particular, Pt σ-acetylide oligomers and polymers have received considerable attention recently in this regard from both applied and fundamental standpoints. Introduction of Pt into a conjugated system allows triplet-state emission,[2] and as a result, Pt-alkynyl oligomers and polymers are ideal for use in organic photocells,[3] light-emitting diodes,[2] and models for triplet manifold studies of conjugated polymers.[4] From a more fundamental view, the delocalization through the Pt center in such mixed metal-organic hybrids has been studied by a number of groups.[5,6] This was very recently quantified in a Pt-alkynyl charge-transfer system by Marder et al. to be only slightly less efficient than a benzene moiety,[7] which bodes well for materials applications for this class of metallamacromolecules.

As part of our continuing efforts to explore and expand the potential materials uses of dehydrobenzoannulenes (DBAs),[8] we have manipulated the optoelectronic properties of the macrocycles by inclusion of electron donor and/or acceptor groups[9] as well as by incorporation of transition metals into the π-conjugated systems.[6b] The potential for induced polarization of the conjugated network via π-back-bonding as well as a

---

* To whom correspondence should be addressed. E-mail: haley@uoregon.edu.

[1] (a) Nguyen, P.; Gomez-Elipe, P.; Manners, I. *Chem. Rev.* **1999**, *99*, 1515−1548. (b) Cooper, T. M. In *Encyclopedia of Nanoscience and Nanotechnology*; Nalwa, H. S., Ed.; American Scientific Publishers: Stevenson Ranch, CA, 2004; Vol. 10.

[2] (a) Wilson, J. S.; Dhoot, A. S.; Seeley, A. J. A. B.; Khan, M. S.; Köhler, A.; Friend, R. H. *Nature* **2001**, *413*, 828−831. (b) Köhler, A.; Wilson, J. S.; Friend, R. H. *Adv. Mater.* **2002**, *14*, 701−707.

[3] Köhler, A.; Whittmann, H. F.; Friend, R. H.; Khan, M. S.; Lewis, J. *Synth. Met.* **1996**, *77*, 147−150.

[4] (a) Wilson, J. S.; Köhler, A.; Friend, R. H.; Al-Suti, M. K.; Al-Mandaray, M. R. A.; Khan, M. S.; Raithby, P. R. *J. Chem. Phys.* **2000**, *113*, 7627−7634. (b) Wilson, J. S.; Chawdhury, N.; Al-Mandaray, M. R. A.; Younus, M.; Khan, M. S.; Raithby, P. R.; Köhler, A.; Friend, R. H. *J. Am. Chem. Soc.* **2001**, *123*, 9412−9417. (c) Liu, Y.; Jiang, S.; Glusac, K.; Powell, D. H.; Anderson, D. F.; Schanze, K. S. *J. Am. Chem. Soc.* **2002**, *124*, 12412−12413. (d) Rogers, J. E.; Cooper, T. M.; Fleitz, P. A.; Glass, D. J.; McLean, D. G. *J. Phys. Chem. A* **2002**, *106*, 10108−10115.

[5] Pt-acetylide oligomers/polymers, inter alia: (a) Sonogashira, K.; Fujikura, Y.; Yatake, T.; Toyoshima, N.; Takahashi, S.; Hagihara, N. *J. Organomet. Chem.* **1978**, *145*, 101−108. (b) Furlani, A.; Licoccia, S.; Russo, M. V.; Chiesi Villa, A.; Guastini, C. *J. Chem. Soc., Dalton Trans.* **1984**, 2197−2206. (c) Harriman, A.; Hissler, M.; Ziessel, R.; De Cian, A.; Fisher, J. *J. Chem. Soc., Dalton Trans.* **1995**, 4067−4080. (d) Onitsuka, K.; Fujimoto, M.; Ohshiro, N.; Takahashi, S. *Angew. Chem., Int. Ed.* **1999**, *38*, 689−692. (e) Back, S.; Albrecht, M.; Spek, A. L.; Rheinwald, G.; Land, H.; van Koten, G. *Organometallics* **2001**, *20*, 1024−1027. (f) Wong, W.; Lu, G.; Choi, K.; Shi, J. *Macromolecules* **2002**, *35*, 3506−3516. (g) Onitsuka, K.; Yabe, K.; Ohshiro, N.; Shimizu, A.; Okumura, R.; Takei, F.; Takahashi, S. *Macromolecules* **2004**, *37*, 8204−8211.

[6] Pt-acetylide macrocycles, inter alia: (a) Faust, R.; Diederich, F.; Gramlich, V.; Seiler, P. *Chem. Eur. J.* **1995**, *1*, 111−117. (b) Pak, J. J.; Weakley, T. J. R.; Haley, M. M. *Organometallics* **1997**, *16*, 4505−4507. (c) Al Quaisi, S. M.; Galat, K. J.; Chai, M.; Ray, D. G., III; Rinaldi, P. L.; Tessier, C. A.; Youngs, W. J. *J. Am. Chem. Soc.* **1998**, *120*, 12149−12150. (d) Bosch, E.; Barnes, C. L. *Organometallics* **2000**, *19*, 5522−5524. (e) Leininger, S.; Olenyuk, B.; Stang, P. J. *Chem. Rev.* **2000**, *100*, 853−908. (f) Siemsen, P.; Gubler, U.; Bosshard, C.; Günter, P.; Diederich, F. *Chem. Eur. J.* **2001**, *7*, 1333−1341. (g) Campbell, K.; McDonald, R.; Ferguson, M. J.; Tykwinski, R. R. *Organometallics* **2003**, *22*, 1353−1355. (h) Kryschenko, Y. K.; Seidel, S. R.; Arif, A. M.; Stang, P. J. *J. Am. Chem. Soc.* **2003**, *125*, 5193−5198.

[7] Jones, S. C.; Coropceanu, V.; Barlow, S.; Kinnibrugh, T.; Timofeeva, T.; Bredas, J.-L.; Marder, S. R. *J. Am. Chem. Soc.* **2004**, *126*, 11782−11783.

[8] Marsden, J. A.; Palmer, G. J.; Haley, M. M. *Eur. J. Org. Chem.* **2003**, 2355−2369.

10.1021/om0490987 CCC: $30.25

Scheme 1

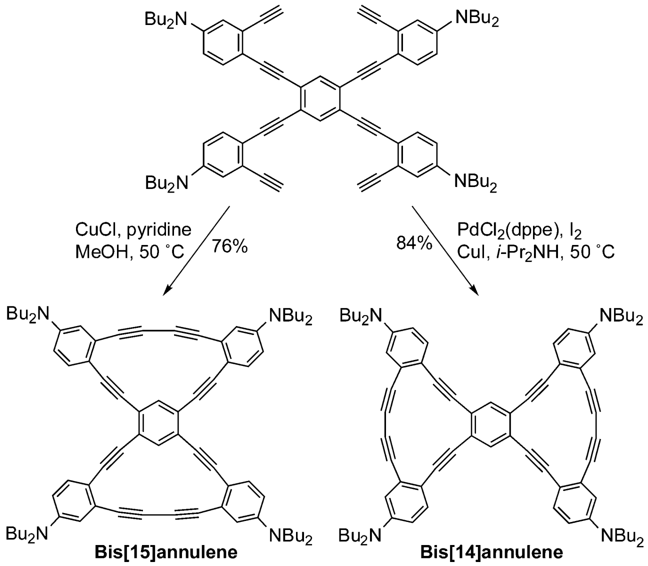

Scheme 2

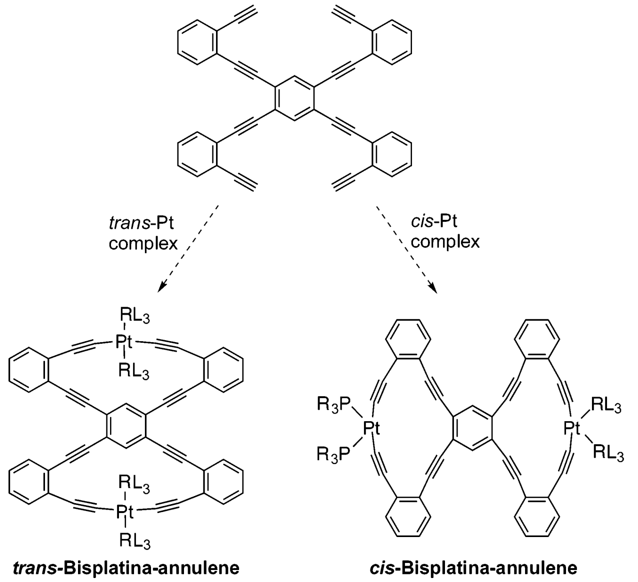

defined directionality usually absent in most organic DBAs are benefits of metal complex inclusion. Additionally, the metal center can serve as an efficient means to introduce stereochemistry via ligand exchange as shown by Tykwinski et al.[10]

We recently reported selectivity for DBA ring formation based on reaction conditions.[11] The geometry of the organometallic intermediate in the final homocoupling reaction was shown to directly affect macrocycle configuration (Scheme 1). Cu-mediated cyclization conditions, which favor a more *trans*-like intermediate, provided excellent selectivity for polyyne cyclization across the *meta*-fused alkynes to produce a bis[15]-annulene. Conversely, the bis[14]annulene was selectively obtained via the cyclization of the *ortho*-fused alkynes of the same precursor using a *cis*-bidendate-ligated Pd catalyst.

The previous results suggest a unique opportunity to generate novel organometallic structures and explore the extent of selectivity via incorporation of oriented metal complexes into the annulene backbone (Scheme 2). Replacement of the cyclization (homocoupling) catalyst with several isomeric Pt metal complexes should favor incorporation of a specific Pt complex isomer into a structure with a similar transition state. Specifically, *trans*-metal complex incorporation should occur with *meta*-substituted α,ω-polyynes and *cis*-metal complex insertion would be favored for *ortho*-substituted α,ω-polyynes. We report herein the synthesis and characterization of seven new platina-annulenes along with their purely hydrocarbon DBA analogues. In addition, we discuss the electronic delocalization in both sets of macrocycles by comparison of their UV−vis spectra.

Results and Discussion

Synthesis of Platina-annulenes. Unlike the chemistry depicted in Scheme 2, we began the synthetic investigation of Pt complex incorporation with α,ω-polyynes that would furnish a single metalla-annulene to confirm feasibility of selective metallacyclization. Production of all seven platina-annulenes originated with known iodoarene **1**.[12] Sonogashira cross-coupling[13] of **1** with trimethylsilylacetylene (TMSA) afforded the differentially silylated diethynylarene **2** in 88% yield (Scheme 3). Treatment of **2** with mild base selectively removed the more labile trimethylsilyl (TMS) group in the presence of the triisopropylsilyl (TIPS) protecting group to afford the free acetylene intermediate.[14] Without further purification, the diyne was cross-coupled with 1,3-diiodobenzene to produce the TIPS-protected α,ω-polyyne **3** in 56% yield. Treatment of **3** with excess Bu_4NF was followed by reaction with Me_3SnNMe_2, replacing the ethynyl hydrogens with more reactive Me_3Sn groups.[15] Addition of stoichiometric *trans*-$PtCl_2(PEt_3)_3$ in the presence of catalytic CuI[16] resulted in transmetalation to form platina-annulene **4** as a yellow solid in 37% yield. [15]Annulene **5** was obtained in 76% yield using Glaser homocoupling conditions[17] after treatment of **3** with Bu_4NF.

Both **4** and **5** are easily distinguished by ^1H NMR spectroscopy due to the enhanced downfield shift of the intraannular benzene proton from 7.74 ppm to 8.70 and 8.69 ppm, respectively.[11] An increased anisotropic

---

[9] (a) Pak, J. J.; Weakley, T. J. R.; Haley, M. M. *J. Am. Chem. Soc.* **1999**, *121*, 8182−8192. (b) Sarkar, A.; Pak, J. J.; Rayfield, G. W.; Haley, M. M. *J. Mater. Chem.* **2001**, *11*, 2943−2945. (c) Marsden, J. A.; Miller, J. J.; Shirtcliff, L. D.; Haley, M. M. *J. Am. Chem. Soc.* **2005**, *127*, 2464−2476.

[10] (a) Campbell, K.; McDonald, R.; Ferguson, M. J.; Tykwinski, R. R. *J. Organomet. Chem.* **2003**, *683*, 379−387. (b) Campbell, K.; Johnson, C. A.; McDonald, R.; Ferguson, M. J.; Haley, M. M.; Tykwinski, R. R. *Angew. Chem., Int. Ed.* **2004**, *43*, 5967−5971.

[11] Marsden, J. A.; Miller, J. J.; Haley, M. M. *Angew. Chem., Int. Ed.* **2004**, *43*, 1694−1697.

[12] Wan, W. B.; Haley, M. M. *J. Org. Chem.* **2001**, *66*, 3893−3901.

[13] (a) Marsden, J. A.; Haley, M. M. In *Metal-Catalyzed Cross-Coupling Reactions*, 2nd ed.; de Meijere, A., Diederich, F., Eds.; Wiley-VCH: Weinheim, 2004; pp 317−394. (b) Sonogashira, K. In *Metal-Catalyzed Cross-Coupling Reactions*; Stang, P. J., Diederich, F., Eds.; VCH: Weinheim, 1997; pp 203−229.

[14] *Protecting Groups in Organic Synthesis*, 3rd ed.; Greene, T. W., Wuts, P. G. M., Eds.; Wiley-VCH: New York, 1999; pp 654−657.

[15] (a) Jones, K.; Lappert, M. F. *J. Chem. Soc.* **1965**, 1944−1951. (b) Jones, K.; Lappert, M. F. *J. Organomet. Chem.* **1965**, *3*, 295−307. (c) Nast, R.; Grouhi, H. *J. Organomet. Chem.* **1980**, *186*, 207−212.

[16] Khan, M. S.; Davies, S. J.; Kakkar, A. K.; Schwartz, D.; Lin, B.; Johnson, B. F. G.; Lewis, J. *J. Organomet. Chem.* **1992**, *424*, 87−97.

[17] Siemsen, P.; Livingston, R. C.; Diederich, F. *Angew. Chem., Int. Ed.* **2000**, *39*, 2632−2657, and references therein.

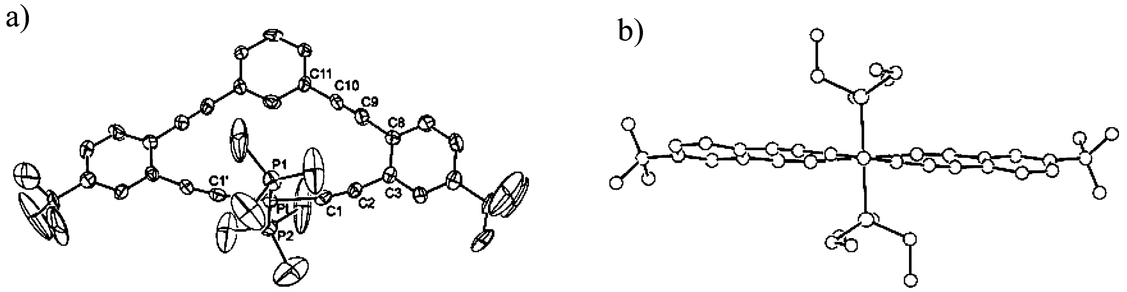

Figure 1. (a) ORTEP of platina-annulene **4**; ellipsoids drawn at the 50% probability level. Selected bond lengths (Å) and angles (deg): Pt−P1 2.291(5), Pt−C1 2.001(15), C1−C2 1.188(19), C9−C10 1.136(18), P1−Pt−P2 172.4(3), C1′−Pt−C1 170.7(8), Pt−C1−C2 169.8(14), C1−C2−C3 168.8(16), C8−C9−C10 173.0(2), C9−C10−C11 178.1(18). (b) View of **4** down [1 0 0] showing nonplanarity and phenyl ring twisting.

Scheme 3

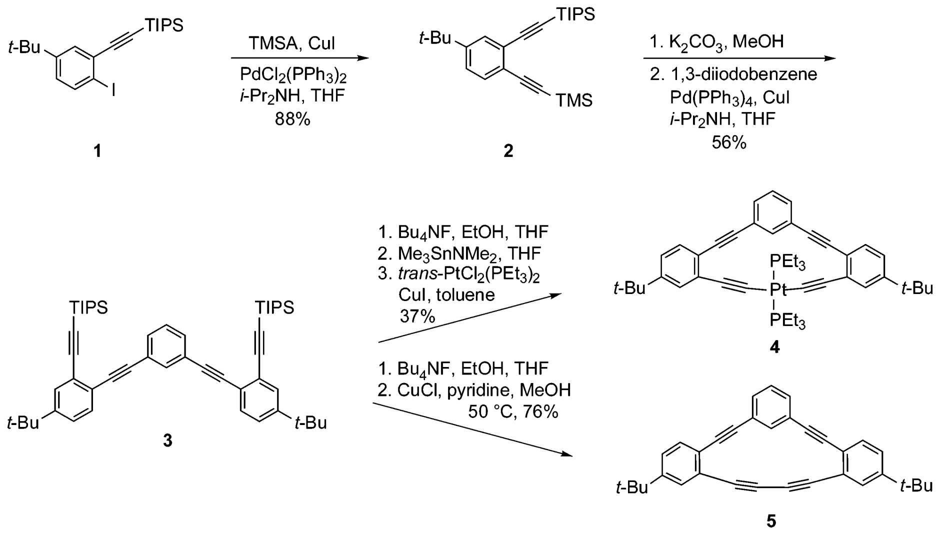

deshielding effect of the ethynyl groups σ-bonded to the Pt complex is responsible for the significant downfield shift. The ^{31}P NMR coupling constant ($J_{\mathrm{P-Pt}}$) of **4** (2328 Hz) is consistent with *trans*-Pt-bis(σ-acetylide) complexes containing PEt$_3$ ligands.[5f,g,6a,f,18a]

Crystals of platina-annulene **4** suitable for X-ray diffraction were obtained by slow diffusion of hexanes into a concentrated THF solution. The ORTEP plot confirms retention of *trans*-geometry for the square planar Pt complex that is doubly σ-bonded to the polyyne backbone (Figure 1). Incorporation of the Pt complex into the annulene backbone results in a distortion from linearity of the σ-bonded ethynyl linkages to the Pt (C1 10.2°, C2 11.2°). The increased strain is also reflected around the Pt center (C1−Pt−C1^{i} 170.7°). Smaller degrees of distortion (C9 7.0°, C10 1.9°) are also observed on the monoyne sides. Despite bond angle distortion, Pt−C and Pt−P bond lengths are consistent with other observed Pt-σ-acetylides.[5,6,8,9,16] Similar to our previously synthesized metalla-annulenes,[6b,19] a distinct nonplanarity of the hydrocarbon ligand is observed. The planes of all three phenyl rings are bent with respect to each other as well as twisted.

To generate platina-annulene **7** and parent [14]-annulene **11**, an *ortho*-substituted isomer of **3** was required. Cross-coupling of diyne **2** to 1,2-diiodobenzene via Sonogashira conditions afforded α,ω-polyyne **6** in 95% yield (Scheme 4). Initial attempts at obtaining **7** containing a *cis*-Pt complex with PEt$_3$ ligands produced two surprising yet undesirable results. The Sn transmetalation conditions successfully used to generate **4** gave a single discreet product in low yield along with copious amounts of oligomeric material. The NMR spectrum of the product gave a 2:1 phosphine ligand to *tert*-butyl proton integration, which was confirmed by single-crystal X-ray diffraction to be bis-Pt-polyyne **8** (Figure 2). In place of the desired second σ-acetylide ligand, both Pt centers of **8** contain iodine, which most certainly originated from the slight excess of CuI. Interestingly, the phosphines on the Pt center have isomerized from *cis* to *trans*, likely so as to incorporate the large iodine atom.

Equally frustrating, the amine-mediated conditions successfully used to generate similar platina-acetylides afforded bis-Pt dimer **9** only.[18] Although the 1:1 phosphine ligand to *tert*-butyl proton ratio in the NMR spectrum was suggestive of monocycle **7**, mass spectrometry and X-ray diffraction correctly elucidated the dimeric structure of **9**. The X-ray structure displayed again an unexpected *trans*-phosphine geometry about the Pt center, as well as an *anti*-relationship between the two central phenyl rings that likely originated from

---

[18] (a) Cross, R. J.; Davison, M. F. *J. Chem. Soc., Dalton Trans.* **1986**, 1987−1992. (b) Sonogashira, K.; Yatake, T.; Tohda, Y.; Takahashi, S.; Hagihara, N. *J. Chem. Soc., Chem. Commun.* **1977**, 291−292.

[19] Pak, J. J.; Darwish, O. S.; Weakley, T. J. R.; Haley, M. M. *J. Organomet. Chem.* **2003**, *683*, 430−434.

Scheme 4

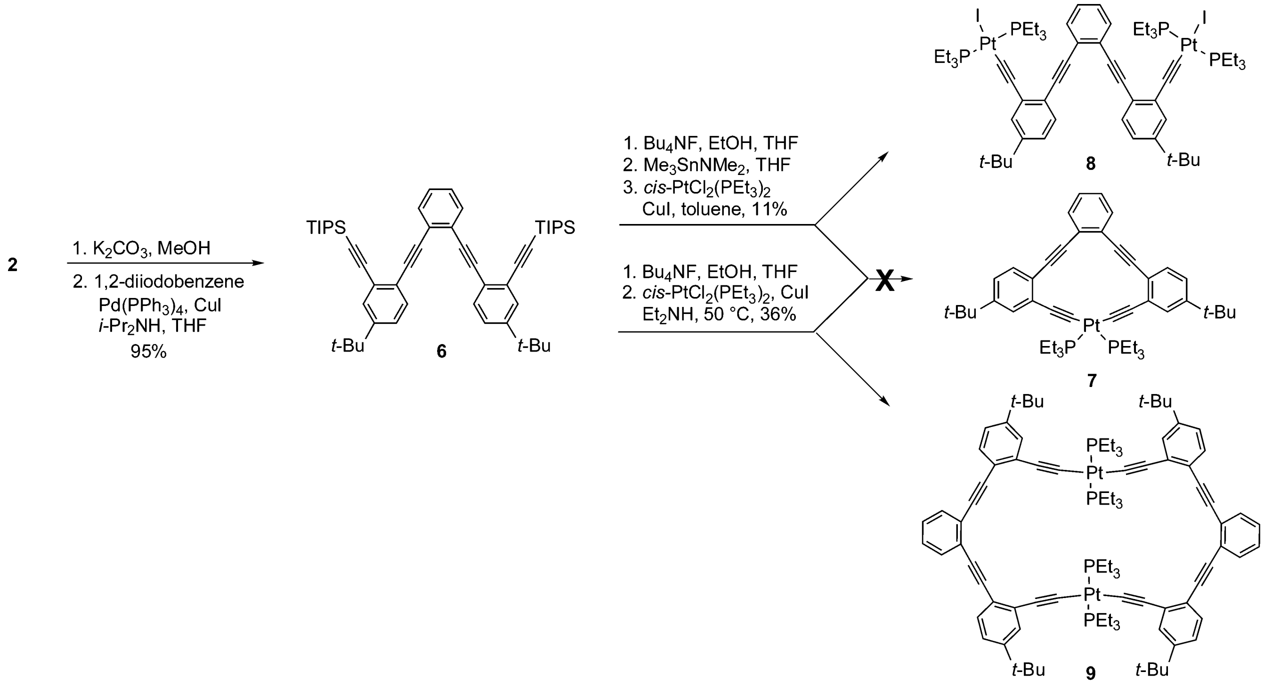

sterics (Figure 3). Analysis of the sp-carbon bond angles showed decreased distortion (0.7−4.6°) in the ethynyl groups compared to **4** and indicated a potential thermodynamic preference over similarly strained **7**. Even with high dilution, the required reaction temperature of 50 °C provided sufficient thermal energy for intermolecular cyclization to effectively compete and produce a structure with less acetylide linkage distortion and thus substantially reduced ring strain.

Although intriguing, the *cis* to *trans* isomerization of the Pt fragments in **8** and **9** is not surprising, as *tran*s bis-acetylides have been shown to be thermodynamically favored over *cis*. CuI has also been suggested to facilitate isomerization via a reversible ethynyl transfer between Pt and Cu.[18] Dimerization or substitution of both ethynyl groups with different Pt complexes is likely favored thermodynamically over cyclization of the strained polyyne **6** due to acetylide linkage distortion and unfavorable entropy associated with steric and torsional interactions from the close proximity of *ortho*-substituted acetylide linkages required for cyclization.

To limit the extent of phosphine isomerization and produce the desired *cis*-platina[15]annulene, we explored use of bulkier ligands, such as PPh_3, as well as bidentate phosphine ligands, such as dppe. Scheme 5 delineates the successful production of platina-annulene **10** with a *cis*-Pt dppe-complex via Sn transmetalation conditions in 52% yield. Synthesis of **10** required several attempts due to the poor solubility of $PtCl_2$(dppe).[20] Optimized conditions for **10** required use of a 1:1 THF/CH_2Cl_2 solvent system and increased reaction time from

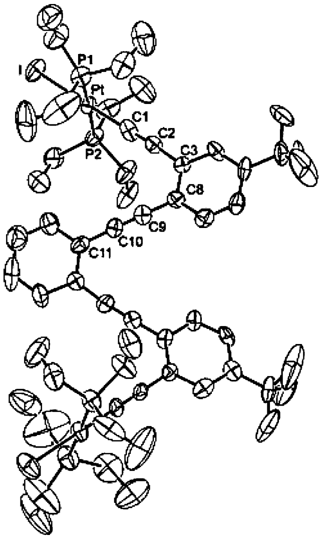

Figure 2. ORTEP of bis-Pt polyyne **8**; ellipsoids drawn at the 50% probability level. Selected bond lengths (Å) and angles (deg): Pt−I 2.655(2), Pt−P1 2.310(8), Pt−C1 1. 88-(2), C1−C2 1.31(3), C9−C10 1.170(3), P1−Pt−P2 175.4-(3), I−Pt−C1 177.0(7), Pt−C1−C2 177.0(2), C1−C2−C3 177.0(3), C8−C9−C10 177.0(3), C9−C10−C11 177.0(3).

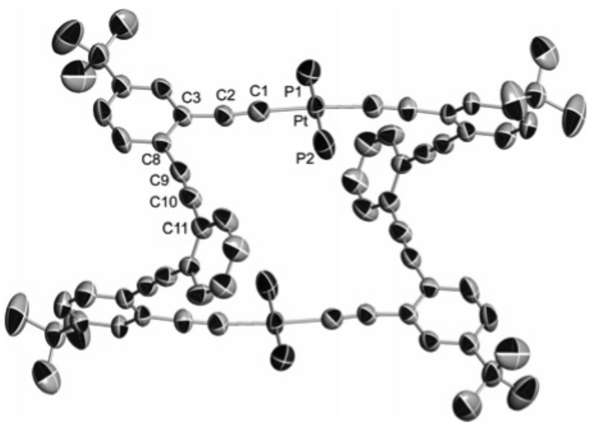

Figure 3. ORTEP of bis-Pt dimer **9**; ellipsoids drawn at the 50% probability level. The phosphine Et groups have been removed for clarity. Selected bond lengths (Å) and angles (deg): Pt−P1 2.280(2), Pt−C1 1.988(8), C1−C2 1.213(9), C9−C10 1.177(9), P1−Pt−P2 176.8(11), C26−Pt−C1 176.5(3), Pt−C1−C2 174.5(7), C1−C2−C3 175.4(8), C8−C9−C10 179.3(9), C9−C10−C11 177.6(8).

Scheme 5

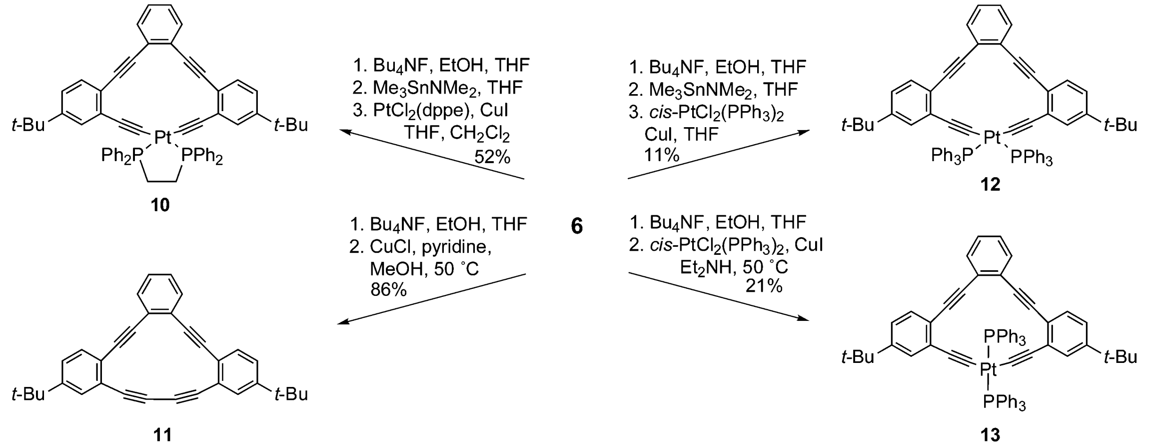

12 to 72 h. Complex **10**, isolated as a fine, colorless solid, displayed a characteristic *cis* $J_{\mathrm{P-Pt}}$ value of 2265 Hz.[10,18] Application of Glaser homocoupling conditions to **6** after removal of the TIPS groups afforded [14]annulene **11** as an orange solid in 86% yield.

In contrast to the $\mathrm{Pt(PEt_3)_2}$-containing complexes, use of $\mathrm{PPh_3}$ as ligand resulted in Pt complex isomerization as well as retention (Scheme 5). Application of Sn transmetalation conditions to **6** afforded the *cis*-platina-annulene **12** in 11% yield. Unexpectedly, amine-mediated metallacyclization produced the *trans* isomer **13** in slightly better yield (21%). In addition to differences in the aromatic region of the ^{1}H NMR spectra, the $J_{\mathrm{P-Pt}}$ value was the most distinguishing analytical difference between **12** and **13**. Cycle **13** displayed a large $J_{\mathrm{P-Pt}}$ value of 2617 Hz, indicative of *trans*-Pt acetylide complexes with $\mathrm{PPh_3}$ ligands, while **12** showed a characteristic *cis*-value of 2333 Hz.[10,18] Temperature and ligand identity appear to be key factors in isolation of stereoisomers **12** and **13**. In contrast to $\mathrm{PEt_3}$, the steric bulk of $\mathrm{PPh_3}$ likely limits access for Cu-mediated isomerization. Likewise, elevated temperature provides increased thermal energy that favors rearrangement to the more stable *trans*-Pt configuration. The dimerization of **6** to **9** is also supported by these conclusions.

In contrast to the planar **11**,[21] the crystal structures of **10** (Figure 4) and **12** (Figure 5) show that metallacyclization results in a nonplanar, saddle-shaped structure, which is the result of the *cis*-orientation of acetylide ligands and *ortho*-substitution of the central benzene ring. The distortions of ethynyl groups σ-bonded to the Pt center (**10**: C1 7.0°, C2 7.2°; **12**: C1 4.7°, C2 5.1°) are reduced compared to **4**.

Attempts to date have not yielded crystals of **13** suitable for X-ray diffraction; however, spectroscopic data highly suggest a planar *trans*-platina-annulene monocycle similar to **4**. This interpretation is supported by marked ^{1}H NMR differences from saddle-like **12**, which results from differential anisotropy due to phenyl ring orientation, as well as the presumed *trans*-orientation of the Pt center based on the large $J_{\mathrm{P-Pt}}$ value (2617 Hz). Semiempirical geometry optimization displays a near planar structure for **13** with maximum acetylide ligand distortion of 10° for the ethynyl groups bonded to the Pt and 8° for the all-carbon ethynyl side.[22]

Synthesis of Bisplatina-annulenes. Successful synthesis of **4**, **10**, **12**, and **13** allowed application of the experimentally determined selectivity principles to an α,ω-polyyne precursor with the potential to form two *cis*- or *trans*-Pt-acetylide complexes based on differential acetylide ligand fusion (Scheme 2). The resultant compound, a bisplatina-annulene, consists of two Pt complexes with phenyl-acetylide ligands in either an *ortho*- or *meta*-relationship on a central benzene ring. Synthesis began with deprotection of diethynyl arene **2** and subsequent Pd cross-coupling to 1,2,4,5-tetraiodobenzene to afford **14** (78%) (Scheme 6). Bisplatina-annulene **15** (21%), containing two *trans*-Pt complexes with $\mathrm{PEt_3}$ ligands, was successfully produced via $\mathrm{Bu_4NF}$ deprotection and amine-mediated metallacyclization of **14**. Compared to monocycle **4**, the intraannular protons of

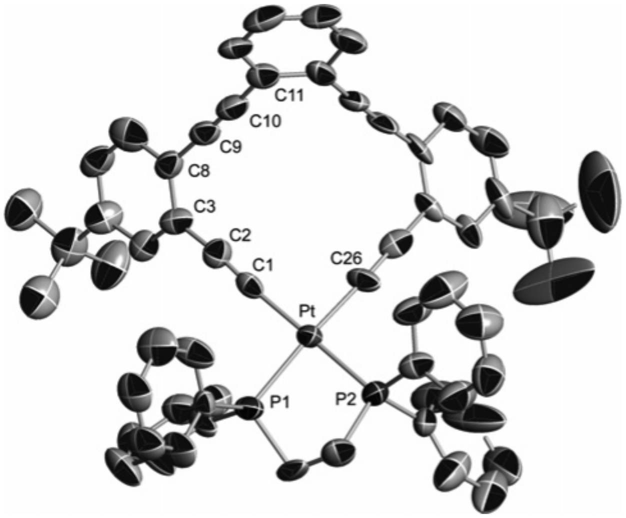

Figure 4. ORTEP of platina-annulene **10**; ellipsoids drawn at the 50% probability level. Selected bond lengths (Å) and angles (deg): Pt−P1 2.270(4), Pt−C1 1.938(14), C1−C2 1.262(17), C9−C10 1.153(18), P1−Pt−P2 85.8(15), C26−Pt−C1 87.6(6), Pt−C1−C2 173.0(14), C1−C2−C3 172.8(17), C8−C9−C10 177.4(19), C9−C10−C11 176.7(19).

---

(20) $\mathrm{PtCl_2(dppe)}$ was synthesized in 2 steps from $\mathrm{PtCl_4}$. See: (a) Clark, H. C.; Manzer, L. E. *J. Organomet. Chem.* **1973**, *59*, 411−428. (b) Anderson, G. K.; Clark, H. C.; Davies, J. A. *Inorg. Chem.* **1981**, *20*, 3607−3611.

(21) The planarity of **5** and **11** is assumed based on X-ray crystal structures of two closely related annulenes; see: (a) Baldwin, K. P.; Matzger, A. J.; Scheiman, D. A.; Tessier, C. A.; Vollhardt, K. P. C.; Youngs, W. J. *Synlett* **1995**, 1215−1218. (b) Tobe, Y.; Kishi, J.; Ohki, I.; Sonoda, M. *J. Org. Chem.* **2003**, *68*, 3330−3332.

(22) Modeled with Spartan Version 5.1.3 (MM3 or AM1 calculations) on a Silicon Graphics Octane workstation.

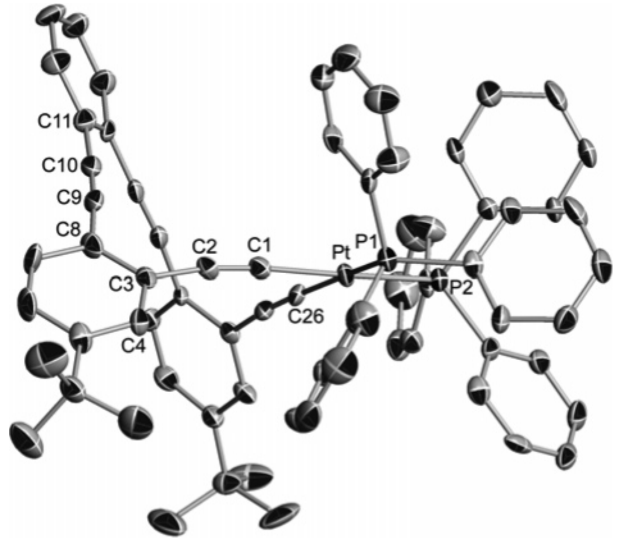

Figure 5. ORTEP of platina-annulene **12**; ellipsoids drawn at the 50% probability level. Selected bond lengths (Å) and angles (deg): Pt−P1 2.313(18), Pt−C1 1.964(7), C1−C2 1.220(9), C9−C10 1.197(9), P1−Pt−P2 100.2(6), C26−Pt−C1 86.0(3), Pt−C1−C2 175.3(6), C1−C2−C3 174.9(7), C8−C9−C10 174.9(7), C9−C10−C11 171.6(8).

15 (8.58 ppm) were shifted slightly upfield (0.13 ppm) and indicative of decreased phenyl ring anisotropy. The J_{P-Pt} value (2325 Hz) was consistent with **4** and previously published *trans*-$PtCl_2(PEt_3)_2$ complexes.[5f,g,6a,f,18a]

The X-ray crystal structure of **15** (Figure 6) showed bond angle lengths and distortions comparable to **4**. In contrast to **4**, however, **15** did not display phenyl ring twisting but instead showed a nonplanar bending similar to a banana (Figure 6b). Single-crystal X-ray diffraction also showed two distinctive stacking patterns of **15** in the same crystal: face to face and edge to face, resultant of favorable ligand−ligand and *tert*-butyl−ligand interactions (Figure 6c).

As with failure to produce **7**, reaction of **14** with *cis*-$PtCl_2(PEt_3)_2$ under amine-mediated metallacyclization conditions resulted in isolation of **15** instead of **16**. In contrast to **8** and **9**, isomerization of the Pt complex and formation of the more stable **15** is the likely result over dimerization or extended linear structures, as the less strained *trans*-bisplatina-annulene can originate from the same precursor. On the basis of successful synthesis of **10**, $PtCl_2$(dppe) was substituted for *cis*-$PtCl_2(PEt_3)_2$ in an attempt to isolate bisplatina-annulene **17**, containing a *cis*-Pt center with *ortho*-fused acetylide ligands (Scheme 7). Application of both metallacyclization methods surprisingly provided bisplatina-annulene **18**, containing two *cis*-Pt complexes, as the major product in 20% and 13% yields. Cycle **18** displayed the most significant intraannular proton downfield shift (9.19 ppm) of all *meta*-fused platina-annulenes. The *cis*-metal complex resulted in closer proximity of acetylide ligands to the intraannular proton and increased anisotropic deshielding. Similar to **10**, **18** displayed a characteristic *cis* J_{P-Pt} value (2230 Hz) in the ^{31}P NMR spectrum.[10,18] Application of Glaser coupling conditions to **14** afforded the parent bis-DBA **19** (39%).

Consistent with ^1H NMR spectroscopy, single-crystal X-ray diffraction of **18** (Figure 7) showed *meta*-fusion of ethynyl substituents and retention of *cis*-Pt orientation. The largest acetylide ligand distortion of all the platina-annulenes is displayed in the monoyne sides of **18** (C9 5.6°, C10, 11.1°) and is the result of *meta*-substitution of the central benzene ring. Contrary to the planar **15**, *cis*-bisplatina-annulenes can display a *syn*- or *anti*-relationship between Pt complexes. The *anti*-relationship, slightly favored by 1 kJ mol^{-1} from molecular mechanics modeling, was isolated as the only cyclized product (Figure 7b).[22]

Complex **18** appeared to directly conflict with our previous assertion of selectivity based on transition-state geometry.[11] Detailed comparison of platina-annulenes and bis-DBAs in Scheme 1 elucidated two key concepts that rationalize **18**. First, DBA cyclization occurs with mix-matched substrate and catalyst geometry but in significantly lower yields.[11] Therefore, a *cis*-Pt complex could be inserted into a *meta*-substituted polyyne, a *trans*-favored substrate for DBA cyclization. Second, the inclusion of an additional atom into the annulene backbone appears to induce significant structural alterations compared to the annulene system depicted in Scheme 1a. Previously synthesized [14]-

Scheme 6

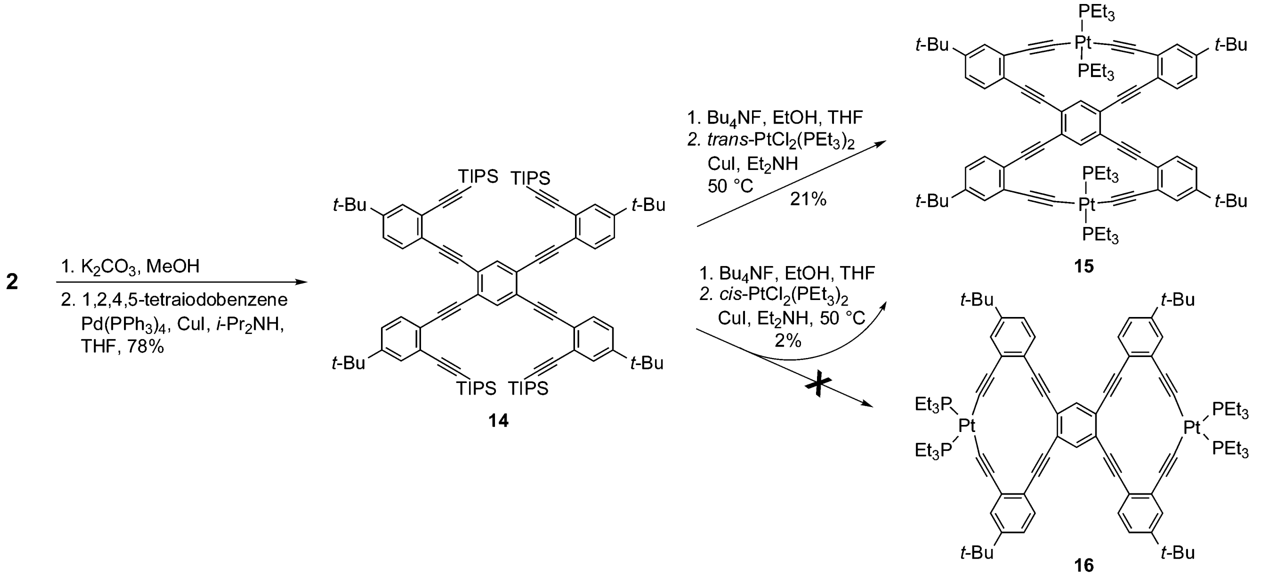

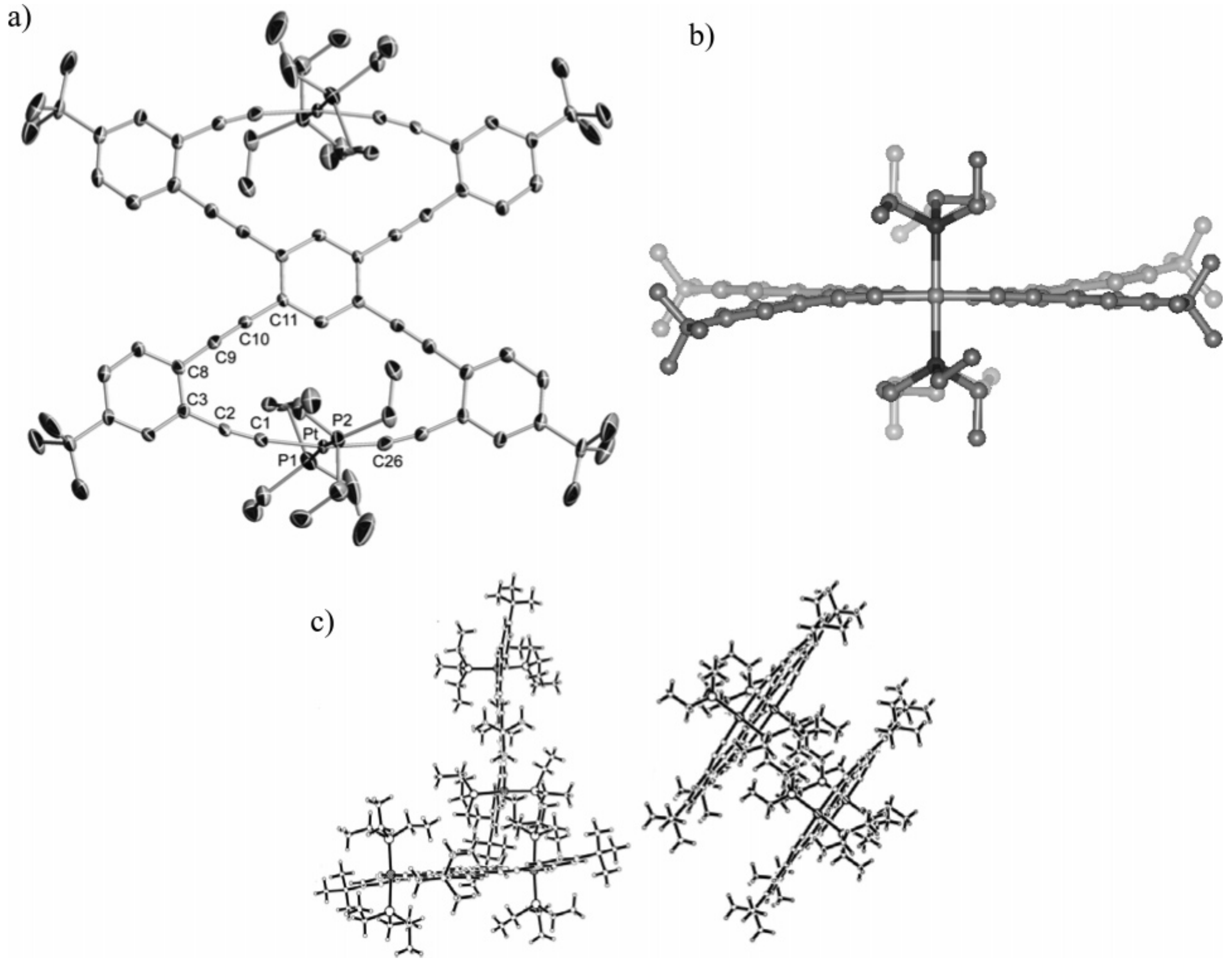

Figure 6. (a) ORTEP of bisplatina-annulene **15**; ellipsoids drawn at the 50% probability level. Selected bond lengths (Å) and angles (deg): Pt−P1 2.289(12), Pt−C1 2.004(4), C1−C2 1.202(5), C9−C10 1.201(5), P1−Pt−P2 174.4(4), C26−Pt−C1 170.9(17), Pt−C1−C2 170.9(4), C1−C2−C3 170.9(4), C8−C9−C10 177.8(5), C9−C10−C11 177.2(5). (b) View of **15** down the [1 1 1] plane showing nonplanarity of the metallamacrocycle but lack of phenyl ring twisting. (c) Molecular stacking of **15** down the [−1 1 0] plane.

annulenes with different alkyl substituents are highly planar,[8,21a] whereas platinacycle variants such as **10** and **12** are bent. Subsequent molecular mechanics geometry optimization illustrates that *cis*-**18** is thermodynamically favored over *cis*-**17** by 36 kJ mol^{-1}.[22]

Platinum Complex Geometry. Comparison of Pt−P and Pt−C bond angles with $J_{\mathrm{P-Pt}}$ values shows a correlation between nonplanarity and decreased $J_{\mathrm{P-Pt}}$ (Table 1). *cis*-Pt complexes characteristically display lower $J_{\mathrm{P-Pt}}$ values than *trans*-complexes with the magnitude dependent on ligand identity (PEt_3 or PPh_3).[5,6,10,18] Compounds **4** and **15**, which displayed the largest acetylide ligand distortion for *trans*-bisethynyl Pt complexes with PEt_3 ligands, were associated with smaller $J_{\mathrm{P-Pt}}$ values than the less strained dimer **9**. The lower $J_{\mathrm{P-Pt}}$ values of **4** and **15** can therefore be linked to a *syn*-like ligand distortion resulting from ring strain. This assertion is confirmed by our previously synthesized *trans*-platina-annulene ($J_{\mathrm{P-Pt}}$ = 2344 Hz) that displayed less ring strain and thus smaller ethynyl distortion.[6b] For the *cis*-platina-annulenes, nonbidentate complex **12** displayed the largest characteristically *cis*-$J_{\mathrm{P-Pt}}$ value resultant from significant PPh_3 ligand and ring strain induced distortion (5−10°). As expected, **10** and **18** showed the lowest *cis*-$J_{\mathrm{P-Pt}}$ value due to the bidentate dppe ligand.

Spectroscopic and Physical Properties. The materials properties of the platina-annulenes were explored to elucidate possible enhanced optical properties beyond those of the parent DBAs. The key issue we sought to discover was the result of transition metal complex incorporation on conjugation and electron delocalization. The amount of delocalization can be qualitatively observed by comparing the electronic absorption spectra of similar substructures. The mono-Pt-annulenes (**4**, **10**, **12**, and **13**) exhibited hypsochromic shifts and $\lambda_{\max}$ decreases compared to their respective DBA analogues (Figure 8). Cycles **10** and **12** (80 nm) showed a more significant $\lambda_{\max}$ decrease compared to **5** (15 nm), which likely resulted from the increased nonplanarity and ring strain of the platina-annulenes. The hypsochromic shift, indicative of decreased electron delocalization, coincides with previously reported platina-acetylide oligomers and small molecules.[6f] The platina-annulenes also displayed a significant decrease in charge-transfer absorptions compared to parent annulenes.

Bisplatina-annulenes **15** and **18**, however, both exhibited bathochromic shifts compared to **19** (Figure 8). Cycle **15** displayed the most significant bathochromic shift (23 nm), and **18** showed the largest $\lambda_{\max}$ value (ca. 105 000 L mol^{-1} cm^{-1}). Additionally, **15** and **18** showed enhanced absorption in the charge-transfer region

Scheme 7

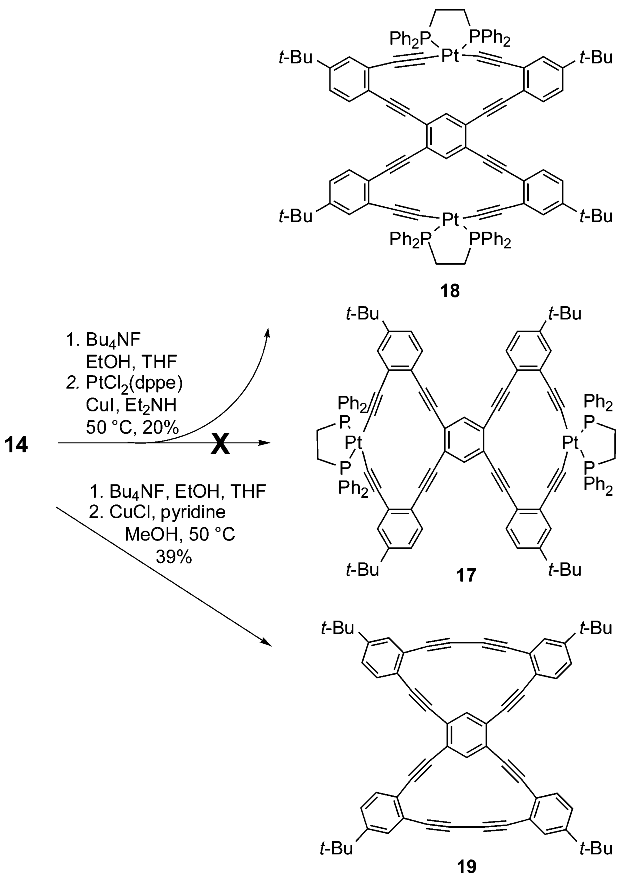

compared to DBA **19**. Diederich et al. have shown that despite efficient metal to ligand charge transfer exhibited by some highly conjugated platina-acetylides, electronic conjugation is localized in the acetylide ligands due to the insulating nature of the Pt atom.[6a,f] A key structural difference of the most red-shifted platina-annulene (**15**) was its planarity. In contrast to hypsochromically shifted monocycle **4**, **15** lacked any significant phenyl ring twisting, as shown by X-ray diffraction. Highly planar annulenes display increased electronic properties in relation to distorted ones.[8,21]

All platina-annulenes exhibited a significant qualitative loss in fluorescence compared to their free acetylene precursors and parent DBAs when visualized in solution or via TLC. Studies on monocycle **4** and bis-Pt-annulene **15** provided fluorescence quantum yield values less than 1%; thus, analysis of the remaining structures was not attempted. Although practically advantageous for determination of starting material consumption, the loss in fluorescence could be attributed to less efficient π-electron delocalization due to the insulating nature of the Pt atom.[6f]

Comparison of platina-annulenes and DBA analogues via DSC indicated a noticeable difference in phase change and associated exotherm. DBAs **5** and **11** exhibited a sharp (2−4 °C) exotherm at ~250 °C that released 0.22 and 0.44 kJ mol^{-1}, respectively. In contrast, the platina-annulenes displayed broad, multistage decomposition above 200 °C. The more strained 15-membered cycles **10**, **12**, and **13** displayed larger exothermic release compared to 16-membered **4**. Metallacycles **10** and **13** displayed the most significant exotherms (7.1 kJ/mol at 417 °C and 10.3 kJ/mol at 413 °C). For the bisplatina-annulenes, **15** exhibited a greater exotherm than **18**, which provides additional insight into the thermodynamic stability of the mismatched *cis*-bisplatina-annulene. The exothermic trends described above and the stability of the platina-annulenes above 200 °C could potentially support a materials application which requires either a specific or tailored energy release.

Conclusions

In summary, we have demonstrated the selective synthesis of seven new platinacycles via Sn transmetalation and amine-mediated oxidative addition. Selectivity hypotheses based on DBA synthesis did not accurately account for the experimentally determined competing factors of ligand identity, Pt complex geometry, reaction conditions, and incorporation of an additional atom into the annulene skeleton. Bulky ligands, such as PPh_3, appeared to limit isomerization, and bidentate phosphine ligands prevented isomerization altogether. The more selective Sn transmetalation conditions limited Pt complex isomerization over the required temperature of the amine-mediated oxidative insertion conditions. For highly strained systems, such as the platina-annulenes **10** and **13**, nonbidentate *cis*-Pt complexes tended to isomerize to the more stable *trans*. Based on experimental results, the most selective metallacyclization method included use of Sn transmetalation conditions and a bidentate Pt complex for *cis*-platina-acetylides, as ligand identity was shown to be less important for *trans*-platina-acetylides. Future studies in this area will focus on heterocyclic and tris-ligated platina-annulenes.

Experimental Section

General Procedures. ^{1}H, ^{13}C, and ^{31}P NMR spectra were recorded using a Varian Inova 300 (^{1}H 299.95 MHz, ^{13}C 75.43 MHz, ^{31}P 121.42 MHz) or Inova 500 (^{1}H 500.10 MHz, ^{13}C 125.75 MHz, ^{31}P 202.44 MHz) spectrometer. Chemical shifts (δ) are expressed in ppm downfield from tetramethylsilane using the residual nondeuterated solvent as internal standard ($CDCl_3$: ^{1}H 7.26 ppm, ^{13}C 77.0 ppm; THF-d_8: ^{1}H 3.58 ppm, ^{13}C 67.57 ppm; o-$C_6D_4Cl_2$: ^{1}H 7.19 ppm). Coupling constants are expressed in hertz. IR spectra were recorded using a Nicolet Magan-FTIR 550 spectrometer. UV−vis were recorded using a Hewlett-Packard 8453 spectrophotometer. Mass spectra were recorded using an Agilent 1100 Series LC/MSD. Elemental analyses were performed by Robertson Microlit Laboratories. Melting points were determined on a Meltemp II apparatus or using a TA Instruments DSC 2920 Modulated DSC and are uncorrected. CH_2Cl_2 was distilled from CaH_2 under a N_2 atmosphere prior to use. THF was purified using an Innovative Technologies solvent system. Et_2NH was distilled prior to use. All other chemicals were of reagent grade and used as obtained from manufacturers. Reactions were carried out in an inert atmosphere (dry N_2 or Ar) when necessary. Column chromatography was performed on Whatman reagent grade silica gel (230−400 mesh). Rotary chromatography was performed on a Harrison Research Chromatotron model 7924T with EM-Science 60PF$_{254}$ silica gel. Precoated silica gel plates (Sorbent Technology, UV$_{254}$, 200 μm, 5 × 20 cm) were used for analytical thin-layer chromatography.

General Metallacyclization Procedure A. A solution of α,ω-polyyne (1 equiv), Bu_4NF (3−5 equiv), and 2−3 drops MeOH in THF (10 mL per 0.1 mmol polyyne) was stirred at room temperature and monitored by TLC until completion

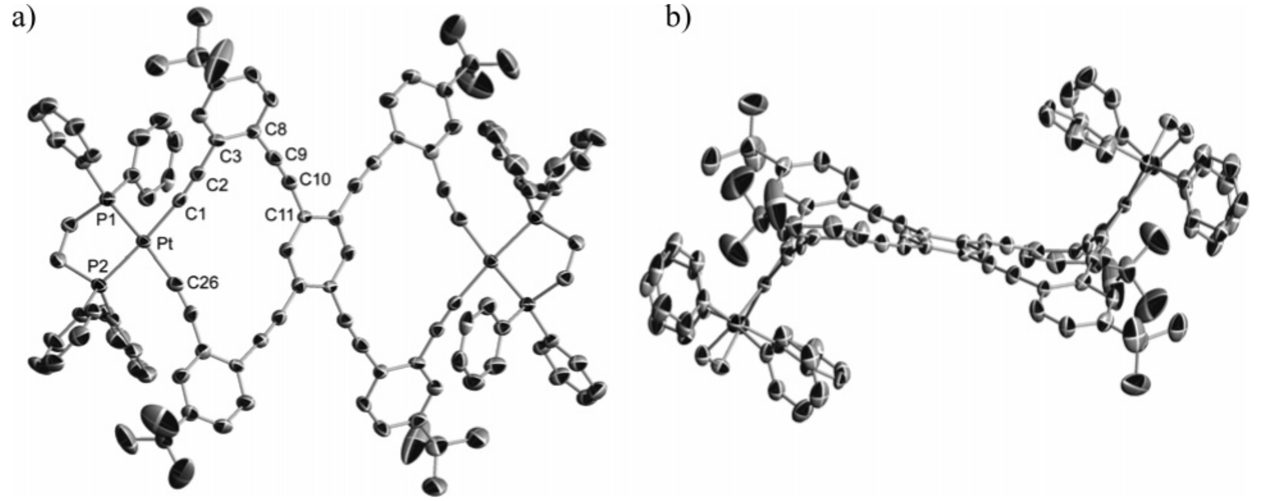

Figure 7. (a) ORTEP of bisplatina-annulene **18**; ellipsoids drawn at the 50% probability level. Selected bond lengths (Å) and angles (deg): Pt−P1 2.284(2), Pt−C1 2.025(9), C1−C2 1.196(11), C9−C10 1.201(11), P1−Pt−P2 86.8(8), C26−Pt−C1 95.8(3), Pt−C1−C2 172.5(7), C1−C2−C3 176.6(9), C8−C9−C10 174.4(9), C9−C10−C11 168.9(8). (b) Side view of ORTEP showing *anti*-orientation of the Pt metal centers.

Table 1. Comparison of Phosphine Ligand, Pt Isomer, ^{31}P NMR Chemical Shift, J_{P-Pt} Value, and Selected Bond Angles for Platinum Complexes 4, 8−10, 12, 13, 15, and 18

compd	ligand	Pt isomer	^{31}P NMR (δ) (J_{P-Pt}, (Hz))	P1−Pt−P2 (deg)	X−Pt−C1 (deg)	Pt−C1−C2 (deg)
4	PEt$_3$	*trans*	10.49 (2328)	172.4	170.7[a]	169.8
8	PEt$_3$	*trans*	9.66 (2311)	175.4	177.0[b]	177.0
9	PEt$_3$	*trans*	12.09 (2360)	176.8	176.5[c]	174.5
10	dppe	*cis*	41.52 (2265)	85.8	87.6[d]	173.0
12	PPh$_3$	*cis*	17.80 (2333)	100.2	86.0[d]	175.3
13	PPh$_3$	*trans*[e]	19.43 (2617)	NA[f]	NA[f]	NA[f]
15	PEt$_3$	*trans*	10.63 (2325)	174.4	170.9[c]	170.9
18	dppe	*cis*	42.43 (2230)	86.8	95.8[c]	172.5

[a] X = C1′. [b] X = I. [c] X = C26; centrosymmetric plane bisects central phenyl ring. [d] X = C26; molecule is not centrosymmetric. [e] Assignment based on NMR and MS. [f] Unable to obtain crystal structure.

(15−30 min). The solution was diluted with Et$_2$O and washed with water and brine. The organic layer was dried over MgSO$_4$ and concentrated in vacuo. Without further purification, the residue was dissolved in THF (20 mL per 0.1 mmol polyyne), and Me$_3$SnNMe$_2$ (1 equiv per polyyne free acetylene functionality) was added. The solution was stirred at room temperature for 2 h and then concentrated in vacuo. Without further purification, the resultant brown oil was combined with PtCl$_2$(PR$_3$)$_2$ (1 equiv) and CuI (10 mol %) and placed under Ar. Deoxygenated solvent (toluene, THF, or CH$_2$Cl$_2$; 25 mL per 0.1 mmol polyyne) was delivered via cannula, and the suspension was stirred under N$_2$ for 12 h at room temperature. The reaction mixture was concentrated by rotary evaporation, and the desired product was purified by column chromatography on silica gel or by Chromatotron.

General Metallacyclization Procedure B. A solution of α,ω-polyyne (1 equiv), Bu$_4$NF (3−5 equiv), and 2−3 drops MeOH in THF (10 mL per 0.1 mmol polyyne) was stirred at room temperature and monitored with TLC until completion (15−30 min). The solution was diluted with Et$_2$O and washed with water and brine. The organic layer was dried over MgSO$_4$ and concentrated in vacuo. Without further purification, the residue was combined with PtCl$_2$(PR$_3$)$_2$ (1 equiv) and CuI (10 mol %) and placed under an Ar environment. Deoxygenated Et$_2$NH (200 mL per 0.1 mmol polyyne) was delivered via cannula, and the suspension was stirred under N$_2$ for 12 h at 50 °C. The reaction mixture was diluted with CH$_2$Cl$_2$ and washed with saturated NH$_4$Cl solution until neutral pH. The organic layer was dried over MgSO$_4$ and concentrated by rotary evaporation. The desired product was purified by column chromatography on silica gel or by Chromatotron.

1-*tert*-Butyl-3-(2-triisopropylsilylethynyl)-4-(2-trimethylsilylethynyl)benzene (12). Iodoarene **1**[9] (9.00 g, 20.4 mmol), CuI (388 mg, 2.04 mmol), and PdCl$_2$(PPh$_3$)$_2$ (717 mg, 1.02 mmol) were combined in THF (100 mL) and *i*-Pr$_2$NH (100 mL). The suspension was deoxygenated by bubbling with Ar, and TMSA (5.65 mL, 40.8 mmol) was added via syringe. The suspension was stirred for 12 h at room temperature under N$_2$. The solvent was removed by rotary evaporation, and the residue was redissolved in Et$_2$O. The organic layer was washed with 10% HCl solution and then neutralized with saturated NaHCO$_3$ and NaCl solution until neutral pH. The organic layer was dried with MgSO$_4$ and concentrated in vacuo. Chromatography on silica gel (3:1 hexanes/CH$_2$Cl$_2$) afforded **2** (7.36 g, 88%) as a highly viscous orange oil. ^{1}H NMR (300 MHz, CDCl$_3$): δ 7.44 (d, J = 1.7 Hz, 1H), 7.39 (d, J = 8.3 Hz, 1H), 7.25 (dd, J = 8.3, 1.7 Hz, 1H), 1.29 (s, 9H), 1.16 (s, 21H), 0.23 (s, 9H). ^{13}C NMR (75 MHz, CDCl$_3$): δ 151.39, 132.72, 129.65, 125.43, 125.33, 122.85, 105.86, 103.67, 97.27, 93.95, 34.68, 31.03, 18.84, 11.37, 0.02. IR (CCl$_4$): ν 2962, 2866, 2155, 1251 cm^{-1}. MS (CI pos) *m*/*z* (%): 481 (M$^+$ + THF, 100), 410 (M$^+$, 10), 409 (20), 245 (22); C$_{26}$H$_{42}$Si$_2$ (410.78). Anal. Calcd for C$_{26}$H$_{42}$Si$_2$: C, 76.02, H, 10.31. Found: C, 75.88, H, 10.26.

α,ω-Polyyne 3. Ethynylarene **2** (1.19 g, 2.9 mmol) was dissolved in Et$_2$O (10 mL) and MeOH (20 mL). K$_2$CO$_3$ (1.20 g, 8.7 mmol) was added, and the suspension was stirred at room temperature for 2 h. The suspension was diluted with Et$_2$O and washed thrice with water and once with brine. The organic layer was dried over MgSO$_4$ and concentrated in vacuo. Without further purification, a syringe pump was used to deliver a deoxygenated solution of the free acetylene in THF (10 mL) over 12 h to a stirred, deoxygenated suspension of

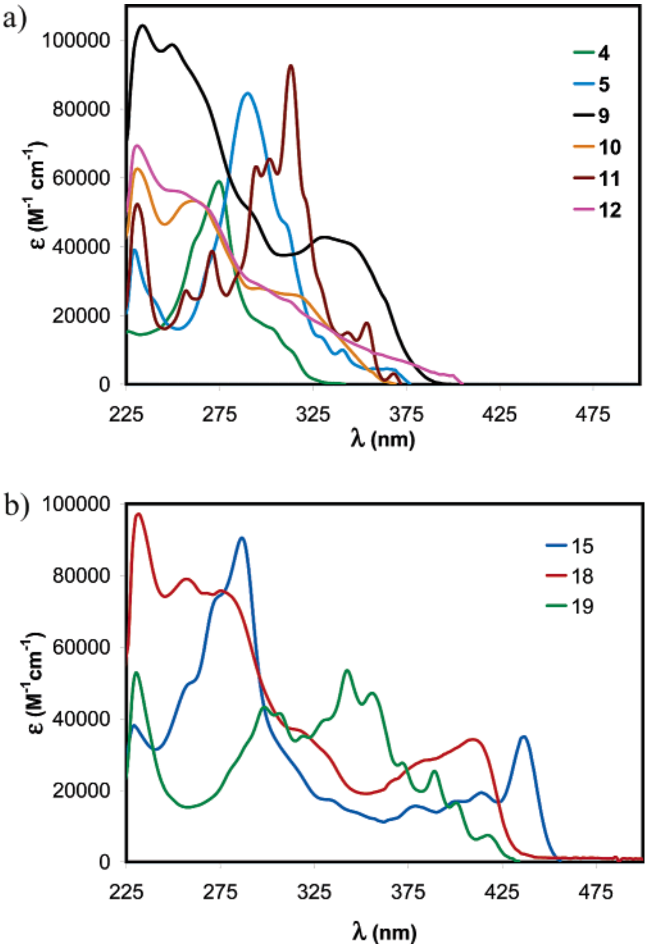

Figure 8. (a) Electronic absorption spectra of platina-annulenes **5**, **9**, **10**, and **12** and DBAs **4** and **11**. (b) Electronic absorption spectra of bisplatina-annulenes **15** and **18** and DBA **19**.

1,3-diiodobenzene (415 mg, 1.26 mmol), $Pd(PPh_3)_4$ (120 mg, 0.15 mmol), and CuI (55 mg, 0.29 mmol) in THF (100 mL) and *i*-Pr_2NH (50 mL). The reaction was stirred an additional 12 h at room temperature under N_2, then the solvent was removed by rotary evaporation. The residue was redissolved in Et_2O, and the organic layer was washed successively with 10% HCl solution and saturated NaCl and $NaHCO_3$ solution until neutral pH. The organic layer was dried with $MgSO_4$ and concentrated in vacuo. Chromatography of the residue on silica gel (hexanes) afforded **3** (533 mg, 56%) as an orange, spongy solid. Mp: 63 °C. ^1H NMR (300 MHz, $CDCl_3$): δ 7.74 (br s, 1H), 7.53 (d, J = 1.8 Hz, 2H), 7.50−7.45 (m, 4H), 7.34 (dd, J = 8.3, 1.8, Hz, 2H), 7.29 (t, J = 7.8 Hz, 1H), 1.34 (s, 18H), 1.16 (s, 42H). ^{13}C NMR (75 MHz, $CDCl_3$): δ 151.32, 135.03, 131.86, 131.17, 129.53, 127.99, 125.49 (2C), 123.68, 122.90, 105.81, 94.24, 91.56, 88.80, 34.69, 31.02, 18.72, 11.36. IR (CCl_4) ν 2962, 2865, 2150, 1495 cm^{-1}. UV/vis (CH_2Cl_2): λ_{max} (ϵ) 225 (42 000), 248 (61 000), 260 (74 000), 304 (33 000), 325 (23 000) nm. MS (CI pos) *m/z* (%): 821 (M^+ + THF, 100), 751 (M^+, 29), 585 (18), 515 (23); $C_{52}H_{70}Si_2$ (751.28). Anal. Calcd for $C_{52}H_{70}Si_2$: C, 83.13, H, 9.39. Found: C, 82.98, H, 9.47.

***trans*-Platina-annulene 4.** Polyyne **3** (113 mg, 0.15 mmol) was reacted with Me_3SnNMe_2 (63 mg, 0.30 mmol) and then *trans*-$PtCl_2(PEt_3)_2$ (63 mg, 0.13 mmol) and CuI (10 mg, 0.05 mmol) in a 1:1 solution of deoxygenated THF/toluene as described in general procedure A. Chromatography on silica gel (2:1 hexanes/CH_2Cl_2) yielded **4** (46.4 mg, 37%) as a light yellow solid. Recrystallization by vapor diffusion with THF/hexanes yielded light, yellow-brown plate crystals. Mp: 284.5 °C (dec). ^1H NMR (300 MHz, $CDCl_3$): δ 8.70 (br s, 1H), 7.40−7.36 (m, 6H), 7.26 (t, J = 7.7 Hz, 1H), 7.13 (dd, J = 8.4, 2.1 Hz, 2H), 2.17−2.07 (m, 12H), 1.32 (s, 18 H), 1.18−1.07 (m, 18H). ^{13}C NMR (75 MHz, $CDCl_3$): δ 150.96, 137.77, 131.78, 130.45, 129.82, 127.96, 125.63, 124.67, 122.92, 121.66, 116.05 (t, J = 14.5 Hz), 109.12, 91.73, 91.12, 34.76, 31.18, 16.30 (t, J = 17.6 Hz), 7.94 (t, J = 11.0 Hz). ^{31}P NMR (121 MHz, $CDCl_3$): δ 10.49 (pseudo-t, J = 2328 Hz). IR (KBr): ν 2962, 2865, 2087, 1384, 1034 cm^{-1}. UV/vis (CH_2Cl_2): λ_{max} (ϵ) 226 (15 000), 275 (58 000), 357 (5000) nm. MS (CI pos) *m/z* (%): 869 (MH^+, 100), 868 (M^+, 65), 531.5 (90); $C_{46}H_{58}P_2Pt$ (867.98). Anal. Calcd for $C_{46}H_{58}P_2Pt$: C, 63.65, H, 6.74. Found: C, 63.49, H, 6.86.

Dehydrobenzo[15]annulene 5. Polyyne **3** (100 mg, 0.13 mmol) was dissolved in THF (10 mL) and treated with MeOH (3 drops) and Bu_4NF (0.5 mL, 1 M THF solution). The solution was stirred for 30 min at room temperature and monitored by TLC. When complete, the reaction mixture was diluted with Et_2O and washed thrice with water and once with brine. The organic layer was then dried with $MgSO_4$ and concentrated in vacuo. Without further purification, the deprotected polyyne was dissolved in THF (10 mL) and added via syringe pump over 24 h to a solution of CuCl (1.31 g, 13.3 mmol) in pyridine (200 mL) and MeOH (50 mL) at 50 °C. The suspension was stirred for an additional 12 h, then the pyridine was removed via rotary evaporation. The resultant thick, green oil was filtered through silica gel (1:1 hexanes/CH_2Cl_2) to remove Cu salts. The filtrate was concentrated in vacuo and recrystallized with THF/hexanes to yield **5** (44 mg, 76%) as a pale yellow solid. Mp: 252.6 °C (dec). ^1H NMR (300 MHz, $CDCl_3$): δ 8.69 (br s, 1H), 7.58 (br s, 2H), 7.41−7.34 (m, 5H), 7.29 (d, J = 1.2 Hz, 2H), 1.33 (s, 18H). ^{13}C NMR (75 MHz, $CDCl_3$): δ 151.60, 144.87, 129.69 (2C), 129.50, 128.61, 127.04, 126.58, 126.00, 124.17, 95.14, 92.29, 82.68, 77.82, 34.84, 30.96. IR (CCl_4): ν 2963, 2867, 2196, 1490 cm^{-1}. UV/vis (CH_2Cl_2): λ_{max} (ϵ) 229 (39 000), 290 (85 000), 341 (10 000) nm. MS (CI pos) *m/z* (%): 579 (M^+ + 2THF, 100), 507 (M^+ + THF, 74), 296 (32); $C_{34}H_{28}$ (436.58). Anal. Calcd for $C_{34}H_{28}\cdot C_4H_8O$: C, 90.44, H, 6.39. Found: C, 90.80, H, 5.98.

α,ω-Polyyne 6. Ethynylarene **2** (1.60 g, 4.05 mmol) was deprotected with K_2CO_3 (1.60 g, 12 mmol) in Et_2O (10 mL) and MeOH (20 mL). K_2CO_3 (1.60 g, 12 mmol) was added, and the suspension was stirred at room temperature for 2 h. The suspension was diluted with Et_2O and washed thrice with water and once with brine. The organic layer was dried over $MgSO_4$ and concentrated in vacuo. Without further purification, a syringe pump was used to deliver a deoxygenated solution of the free acetylene in THF (10 mL) over 12 h to a stirred, deoxygenated suspension of 1,2-diiodobenzene (500 mg, 1.50 mmol), $Pd(PPh_3)_4$ (233 mg, 0.22 mmol), and CuI (76 mg, 0.40 mmol) in THF (150 mL) and *i*-Pr_2NH (100 mL). The reaction was stirred an additional 12 h at room temperature under N_2, then the solvent was removed by rotary evaporation. The residue was redissolved in Et_2O, and the organic layer was washed with 10% HCl solution and then with saturated $NaHCO_3$ and NaCl solution until neutral pH. The organic layer was dried with $MgSO_4$ and concentrated in vacuo. Chromatography of the residue on silica gel (hexanes) yielded **6** (1.08 g, 95%) as an orange, spongy solid. Mp: 121.5 °C. ^1H NMR (300 MHz, $CDCl_3$): δ 7.61 (*AA′*m, 2H), 7.57 (d, J = 1.8 Hz, 2H), 7.54 (d, J = 8.4 Hz, 2H), 7.32 (*BB′*m, 2H), 7.30 (dd, J = 8.4, 1.8 Hz, 2H), 1.38 (s, 18H), 1.20 (s, 42H). ^{13}C NMR (75 MHz, $CDCl_3$): δ 151.15, 132.40, 131.79, 129.43, 127.58, 126.27, 125.41, 125.24, 123.32, 105.98, 94.09, 92.59, 91.48, 34.66, 31.04, 18.74, 11.41. IR (CCl_4): ν 2959, 2864, 2155, 1462 cm^{-1}. UV/vis (CH_2Cl_2): λ_{max} (ϵ) 242 (58 100), 249 (60 000), 257 (56 000), 296 (22 000), 315 (17 000) nm. MS (CI pos) *m/z* (%): 821 (M^+ + THF, 22), 751 (M^+, 100), 585.3 (17), 515 (20); $C_{52}H_{70}Si_2$ (751.28). Anal. Calcd for $C_{52}H_{70}Si_2$: C, 83.13, H, 9.39. Found: C, 82.91, H, 9.50.

Bis-Pt-polyyne 8. Polyyne **6** (75 mg, 0.10 mmol) was reacted with Me_3SnNMe_2 (41 mg, 0.2 mmol) and subsequently *cis*-$PtCl_2(PEt_3)_2$ (68 mg, 0.14 mmol) and CuI (10 mg, 0.05

mmol) in deoxygenated toluene as described in general procedure A. Chromatography on silica gel (2:1 hexanes/CH_2Cl_2) afforded **8** (9.5 mg, 11%) as a dark yellow solid. Recrystallization by vapor diffusion with THF/hexanes yielded light, yellow-brown needles. Mp: 214.9 °C (dec). ^{1}H NMR (300 MHz, $CDCl_3$): δ 7.51 (*AA′*m, 2H), 7.39 (d, J = 8.3 Hz, 2H), 7.35 (d, J = 1.8 Hz, 2H), 7.22 (*BB′*m, 2H), 7.08 (dd, J = 8.3, 1.8 Hz, 2H), 2.24−2.16 (m, 24H), 1.30 (s, 18H), 1.16−1.05 (m, 36H). ^{13}C NMR (75 MHz, $CDCl_3$): δ 150.87, 132.41, 131.77, 130.12, 128.28, 127.34, 126.61, 122.41, 121.23, 99.99, 94.61, 94.52 (t, J = 14.2 Hz), 89.97, 34.58, 31.10, 16.64 (t, J = 10.7 Hz), 8.29. ^{31}P NMR (121 MHz, $CDCl_3$): δ 9.66 (pseudo-t, J = 2311 Hz). IR (CCl_4): ν 2962, 2873, 2105, 1384 cm^{-1}. MS (CI pos) m/z (%): 1623 (M^+ + THF, 15), 1554 (MH^+, 82), 1553 (M^+, 100); $C_{58}H_{88}I_2P_4Pt_2$ (1553.18). Anal. Calcd for $C_{58}H_{88}I_2P_4Pt_2$: C, 44.85, H, 5.71. Found: C 45.07, H 5.54.

***trans*-Platina-annulene Dimer 9.** Polyyne **6** (150 mg, 0.2 mmol) was reacted with *cis*-$PtCl_2(PEt_3)_2$ (100 mg, 0.2 mmol) and CuI (10 mg, 0.04 mmol) as described in general procedure B. Chromatography on silica gel (2:1 hexanes/CH_2Cl_2) and subsequent precipitation with $CHCl_3$ yielded **9** (63 mg, 36%) as a pale yellow solid. Recrystallization by vapor diffusion with THF/hexanes afforded light yellow crystals. Mp: 315.1 °C (dec). ^{1}H NMR (300 MHz, $CDCl_3$): δ 7.50 (*AA′*m, 2H), 7.35 (d, J = 8.3 Hz, 2H), 7.31 (d, J = 1.8 Hz, 2H), 7.21 (*BB′*m, 2H), 7.06 (dd, J = 8.3, 1.8 Hz, 2H), 2.07−2.05 (m, 12H), 1.26 (s, 18H), 1.09−1.03 (m, 18H). ^{13}C NMR (75 MHz, $CDCl_3$): δ 150.48, 132.61, 132.27, 130.48, 128.82, 127.32, 126.42, 121.81, 121.11, 113.27 (t, J = 15.5 Hz), 109.01, 94.31, 89.10, 34.48, 31.08, 16.41 (t, J = 17.6 Hz), 8.50 (t, J = 11.0 Hz),. ^{31}P NMR (121 MHz, $CDCl_3$): δ 12.09 (pseudo-t, J = 2360 Hz). IR (KBr): ν 2962, 2091, 1384 cm^{-1}. UV/vis (CH_2Cl_2): λ_{max} (ϵ) 234 (104 000), 250 (99 000), 331 (43 000) nm. MS (CI pos) m/z (%): 1736 (MH^+, 25), 1735 (M^+, 100), 1617 (13); $C_{92}H_{116}P_4Pt_2$ (1735.96). Anal. Calcd for $C_{92}H_{116}P_4Pt_2$: C, 63.65, H, 6.74. Found: C, 63.61, H, 6.69.

***cis*-Platina-annulene 10.** Polyyne **6** (100 mg, 0.133 mmol) was reacted with Me_3SnNMe_2 (55 mg, 0.27 mmol) and subsequently $PtCl_2$(dppe) (73 mg, 0.11 mmol) and CuI (5 mg, 0.03 mmol) in a 1:1 solution of deoxygenated THF/CH_2Cl_2 as described in general procedure A. Chromatography on silica gel (1:1 hexanes/CH_2Cl_2) yielded **10** (70 mg, 52%) as a fine white solid. Recrystallization by vapor diffusion with $C_6H_4Cl_2$/hexanes yielded colorless crystals. Mp: 229 °C (dec). ^{1}H NMR (300 MHz, THF-d_8): δ 8.14−8.05 (m, 8H), 7.56 (*AA′*m, 2H), 7.41−7.35 (m, 12H), 7.29 (d, J = 8.0 Hz, 2H), 7.24 (*BB′*m, 2H), 7.06 (d, J = 1.9 Hz, 2H), 7.02 (dd, J = 8.0, 1.9 Hz, 2H), 2.56−2.42 (m, 4H), 1.21 (s, 18H). ^{13}C NMR (125 MHz, THF-d_8): δ 151.02, 134.77 (m), 134.02, 132.62, 132.32, 131.90, 131.75, 129.48 (m), 128.87, 128.03, 127.351, 122.98, 122.30, 113.30 (dd, J = 147.5, 14.3 Hz), 110.95 (d, J = 34.0 Hz), 94.60, 90.49, 55.054, 35.22, 31.66. ^{31}P NMR (121 MHz, THF-d_8): δ 41.52 (pseudo-t, J = 2265 Hz). IR (KBr): ν 3054, 2961, 2110, 1436 cm^{-1}. UV/vis (CH_2Cl_2): λ_{max} (ϵ) 231 (62 000), 261 (54 000), 296 (27 000), 305 (25 000) nm. MS (CI pos) m/z (%): 1031 (MH^+, 65), 1030.2 (M^+, 53), 531 (100); $C_{60}H_{52}P_2Pt$ (1030.08). Anal. Calcd for $C_{60}H_{52}P_2Pt\cdot C_6H_4Cl_2$: C, 67.35, H, 4.80. Found: C, 67.55, H, 4.66.

Dehydrobenzo[14]annulene 11. Polyyne **6** (80 mg, 0.11 mmol) was dissolved in THF (10 mL) and treated with MeOH (3 drops) and Bu_4NF (0.5 mL, 1 M THF solution). The solution was stirred for 30 min at room temperature and monitored by TLC. Upon completion, the reaction mixture was diluted with Et_2O (20 mL) and washed thrice with water and once with brine. The organic layer was dried with $MgSO_4$ and concentrated in vacuo. Without further purification, the deprotected polyyne was dissolved in THF (10 mL) and added via syringe pump over 24 h to a solution of CuCl (1.03 g, 10.4 mmol) in pyridine (200 mL) and MeOH (50 mL). The suspension was stirred at 50 °C under N_2 for an additional 12 h, then the pyridine was removed via rotary evaporation. The resultant thick, green oil was filtered through silica gel (1:1 hexanes/CH_2Cl_2) to remove Cu salts, and the filtrate was concentrated by rotary evaporation. Chromatography on silica gel (1:1 hexanes/CH_2Cl_2) afforded **11** (40 mg, 86%) as a pale yellow solid. Mp: 252.3 °C (dec). ^{1}H NMR (300 MHz, $CDCl_3$): δ 7.91 (*AA′*m, 2H), 7.81 (d, J = 8.5 Hz, 2H), 7.63 (d, J = 1.8 Hz, 2H), 7.52 (dd, J = 8.5, 1.8 Hz, 2H), 7.43 (*BB′*m, 2H), 1.37 (s, 18H). ^{13}C NMR (75 MHz, $CDCl_3$): δ 151.39, 135.86, 132.79, 127.74, 126.56, 126.12, 126.04, 123.37, 122.39, 93.13, 93.09, 86.07, 79.68, 34.90, 31.06. IR (CCl_4): ν 2963, 2867, 2150, 1485 cm^{-1}. UV/vis (CH_2Cl_2): λ_{max} (ϵ) 231 (52 000), 271 (39 000), 295 (64 000), 302 (65 000), 313 (93 000) nm. MS (CI pos) m/z (%): 509 (M^+ + THF, 100), 438 (MH^+, 10); $C_{34}H_{28}$ (436.58).

***cis*-Platina-annulene 12.** Polyyne **6** (100 mg, 0.133 mmol) was reacted with Me_3SnNMe_2 (55 mg, 0.27 mmol) and subsequently *cis*-$PtCl_2(PPh_3)_2$ (105 mg, 0.133 mmol) and CuI (5 mg, 0.03 mmol) in a solution of deoxygenated THF as described in general procedure A. Purification on a Chromatotron plate (1 mm, 1:1 hexanes/CH_2Cl_2) yielded **12** (17 mg, 11%) as a pale white solid. Recrystallization by vapor diffusion with $C_6H_4Cl_2$/hexanes yielded colorless crystals. Mp: 187.9 °C (dec). ^{1}H NMR (300 MHz, $CDCl_3$): δ 7.66 (*AA′*m, 2H), 7.51−7.45 (m, 12H), 7.35 (*BB′*m, 2H), 7.24 (d, J = 8.1 Hz, 2H), 7.23−7.17 (m, 6H), 7.11−7.04 (m, 12H), 6.91 (dd, J = 8.1, 1.8 Hz, 2H), 6.57 (d, J = 1.8 Hz, 2H), 1.13 (s, 18H). ^{13}C NMR (75 MHz, $CDCl_3$): δ 149.67, 134.84, 132.10, 131.91, 131.10, 129.81, 128.54, 128.44, 127.81, 127.58, 127.02, 126.43, 122.42, 121.31, 96.11, 93.27, 89.09, 34.32, 31.05. ^{31}P NMR (121 MHz, $CDCl_3$): δ 17.80 (pseudo-t, J = 2333 Hz). IR (KBr): ν 2960, 2115, 1631.16, 1096 cm^{-1}. UV/vis (CH_2Cl_2): λ_{max} (ϵ) 231 (69 000), 258 (57 000), 305 (29 000) nm. MS (CI pos) m/z (%): 1159 (M^+ + 3, 90), 1157 (MH^+, 80), 1021 (100); $C_{70}H_{58}P_2Pt$ (1156.24). Anal. Calcd for $C_{70}H_{58}P_2Pt\cdot 0.5C_6H_4Cl_2$: C, 71.30, H, 4.92. Found: C, 71.43, H, 4.83.

***trans*-Platina-annulene 13.** Polyyne **6** (153 mg, 0.2 mmol) was reacted with *cis*-$PtCl_2(PPh_3)_2$ (160 mg, 0.2 mmol) and CuI (14 mg, 0.08 mmol) as described in general procedure B. Purification on a Chromatotron plate (1 mm, 2:1 hexanes/CH_2Cl_2) and subsequent precipitation with hexanes yielded **13** (50 mg, 21%) as a white powder. Mp: 241.4 °C (dec). ^{1}H NMR (300 MHz, $CDCl_3$): δ 8.00−7.97 (m, 12H), 7.48 (d, J = 8.1 Hz, 2H), 7.31−7.22 (m, 20H), 7.03 (dd, J = 8.1, 1.8 Hz, 2H), 6.47 (d, J = 1.8 Hz, 2H), 6.35 (*BB′*m, 2H), 1.21 (s, 18H). ^{13}C NMR (75 MHz, $CDCl_3$): δ 150.12, 135.39 (t, J = 6.0 Hz), 131.50, 131.12, 130.98, 130.73, 130.12, 127.68 (t, J = 5.0 Hz), 127.52, 127.14, 126.29, 121.39, 120.98, 117.79 (t, J = 15.6 Hz), 114.46, 95.31, 89.27, 34.42, 31.07. ^{31}P NMR (121 MHz, $CDCl_3$): δ 19.43 (pseudo-t, J = 2617 Hz). IR (KBr): ν 2960, 2924, 2854, 2100, 1384, 1110 cm^{-1}. UV/vis (CH_2Cl_2): λ_{max} (ϵ) 232 (50 200), 262 (42 600), 328 (13 200), 353 (12 900), 364 (12 700), 379 (12 600) nm. MS (CI pos) m/z (%): 1195 (M^+ + CH_3CN, 77), 1157 (MH^+, 15), 558 (100); $C_{70}H_{58}P_2Pt$ (1156.24). Anal. Calcd for $C_{70}H_{58}P_2Pt$: C, 72.71, H, 5.06. Found: C, 71.94, H, 5.28.

α,ω-Polyyne 14. Ethynylarene **2** (2.3 g, 5.67 mmol) was dissolved in Et_2O (10 mL) and MeOH (20 mL). K_2CO_3 (2.0 g, 15 mmol) was added, and the suspension was stirred at room temperature for 2 h. The suspension was diluted with Et_2O and washed thrice with water and once with brine. The organic layer was dried over $MgSO_4$ and concentrated in vacuo. Without further purification, a syringe pump was used to deliver a deoxygenated solution of the free acetylene in THF (10 mL) over 24 h to a stirred, deoxygenated suspension of 1,2,4,5-tetraiodobenzene (550 mg, 0.95 mmol), $Pd(PPh_3)_4$ (231 mg, 0.20 mmol), and CuI (76 mg, 0.40 mmol) in THF (200 mL) and *i*-Pr_2NH (100 mL). The reaction was stirred an additional 24 h at room temperature under N_2, then the solvent was removed by rotary evaporation. The residue was redissolved in Et_2O, and the organic layer was washed with 10% HCl solution and then with saturated NaCl and $NaHCO_3$ solution until neutral pH. The organic layer was dried with $MgSO_4$ and concentrated in vacuo. Chromatography of the residue on silica gel (5:1 hexanes/CH_2Cl_2) afforded **14** (1.04 g, 78%) as a light yellow, fine powder. Mp: 219−221 °C. ^{1}H NMR (300 MHz, $CDCl_3$): δ 7.72 (s, 2H), 7.50 (d, J = 1.8 Hz, 4H), 7.46 (d, J = 8.1 Hz, 4H), 7.27 (dd, J = 8.1, 1.8 Hz, 4H), 1.33 (s, 36H), 1.10 (s, 84H). ^{13}C NMR (75 MHz, $CDCl_3$): δ 151.29, 135.42, 132.32, 129.35, 125.43, 125.36, 125.29, 123.04, 105.69, 94.43, 94.02, 90.45, 34.70, 31.04, 18.69, 11.37. IR (CCl_4): ν 2959, 2865, 2154, 1463, 1384 cm^{-1}. UV/vis (CH_2Cl_2): λ_{max} (ϵ) 240 (62 000), 256 (48 000), 269 (50 000), 327 (24 000), 364 (17 500) nm. MS (CI pos) *m/z* (%): 1495 (M^+ + THF, 10), 1425 (MH^+, 100), 1424 (M^+, 93); $C_{98}H_{134}Si_4$ (1424.45). Anal. Calcd for $C_{98}H_{134}Si_4 \cdot 0.5CH_2Cl_2$: C, 80.65, H, 9.28. Found: C, 80.97, H, 9.05.

***trans*-Bisplatina-annulene 15.** Polyyne **14** (150 mg, 0.11 mmol) was reacted with *trans*-$PtCl_2(PEt_3)_2$ (106 mg, 0.21 mmol) and CuI (10 mg, 0.04 mmol) as described in general procedure B. Purification on a Chromatotron plate (1 mm, 1:1 hexanes/CH_2Cl_2) provided **15** (32 mg, 0.02 mmol, 21%) as a pale yellow solid. Recrystallization by vapor diffusion with THF/hexanes afforded light yellow crystals. Mp: 341.4 °C (dec). ^{1}H NMR (300 MHz, $CDCl_3$): δ 8.58 (s, 2H), 7.52 (d, J = 8.2 Hz, 4H), 7.35 (d, J = 1.5 Hz, 4H), 7.21 (dd, J = 8.2, 1.5 Hz, 4H), 2.15−2.11 (m, 24H), 1.34 (s, 36H), 1.18−1.08 (m, 36H). ^{13}C NMR (75 MHz, $CDCl_3$): δ 151.18, 137.61, 131.79, 130.73, 125.52, 124.77, 123.17, 121.87, 116.39 (t, J = 15.0 Hz), 109.29, 96.78, 90.57, 34.84, 31.20, 16.34 (t, J = 17.2 Hz), 7.99. ^{31}P NMR (121 MHz, $CDCl_3$): δ 10.63 (pseudo-t, J = 2325 Hz). IR (CCl_4): ν 2962, 2090, 1498, 1035 cm^{-1}. UV/vis (CH_2Cl_2): λ_{max} (ϵ) 228 (37 000), 286 (90 000), 436 (35 000) nm. MS (CI pos) *m/z* (%): 1658 (MH^+, 8), 1657 (M^+, 6), 585 (35), 531 (100); $C_{86}H_{110}P_4Pt_2$ (1657.84). Anal. Calcd for $C_{86}H_{110}P_4Pt_2$: C, 62.31, H, 6.69. Found: C, 62.56, H, 6.50.

***cis*-Bisplatina-annulene 18.** Polyyne **14** (75 mg, 0.05 mmol) was reacted with $PtCl_2$(dppe) (69 mg, 0.10 mmol) and CuI (5 mg, 0.03 mmol) as described in general procedure B. Purification on a Chromatotron plate (1 mm, 1:1 hexanes/CH_2Cl_2) provided **18** (20 mg, 19%) as a yellow solid. Recrystallization by vapor diffusion with *o*-$C_6H_4Cl_2$/hexanes afforded light yellow crystals. Mp: 351.7 °C (dec). ^{1}H NMR (300 MHz, *o*-$C_6D_4Cl_2$): δ 9.19 (s, 2H), 7.94−7.88 (m, 16H), 7.34−7.24 (m, 28H), 7.02−6.94 (m, 8H), 2.30−2.24 (m, 8H), 1.14 (s, 36H). ^{13}C NMR: insufficient solubility to obtain spectrum. ^{31}P NMR (121 MHz, $CDCl_3$): δ 42.43 (pseudo-t, J = 2230 Hz). IR (CCl_4): ν 2958, 2924, 2091.27, 1384, 1108 cm^{-1}. UV/vis (CH_2Cl_2): λ_{max} (ϵ) 231 (103 000), 257 (84 000), 275 (80 500), 409 (36 000) nm. MS (CI pos) *m/z* (%): 1983 (M^+, 31), 1981 (23), 1426 (70), 1028 (100); $C_{114}H_{99}P_4Pt_2$ (1983.06). Anal. Calcd for $C_{114}H_{99}P_4Pt_2 \cdot 2C_6H_4Cl_2$: C, 66.49, H, 4.69. Found: C, 66.29, H, 4.31.

Bisdehydrobenzo[15]annulene 19. Polyyne **14** (75 mg, 0.05 mmol) was dissolved in THF (10 mL) and treated with MeOH (3 drops) and Bu_4NF (0.5 mL, 1 M THF solution). The solution was stirred for 30 min at room temperature and monitored by TLC. Upon completion, the reaction mixture was diluted with Et_2O and washed thrice with water and once with brine. The organic layer was dried with $MgSO_4$ and concentrated in vacuo. Without further purification, the deprotected polyyne was dissolved in THF (10 mL) and added via syringe pump over 24 h to a solution of CuCl (514 mg, 5.2 mmol) in pyridine (200 mL) and MeOH (50 mL). The suspension was stirred at 50 °C for an additional 12 h, then the pyridine was removed via rotary evaporation. The resultant thick, green oil was filtered through silica gel (1:1 hexanes/CH_2Cl_2) to remove Cu salts, and the filtrate was concentrated by rotary evaporation. Chromatography on silica gel (2:1 hexanes/CH_2Cl_2) afforded **19** (16 mg, 39%) as a yellow solid. Mp: 249.1 °C (dec). ^{1}H NMR (300 MHz, $CDCl_3$): δ 8.43 (s, 2H), 7.92 (d, J = 8.6 Hz, 4H), 7.64 (d, J = 1.9 Hz, 4H), 7.56 (dd, J = 8.6, 1.9 Hz, 4H), 1.38 (s, 36H). ^{13}C NMR (75 MHz, $CDCl_3$): δ 151.95, 143.06, 133.04, 126.27 (3C), 122.76, 122.65, 95.03, 92.32, 86.05, 79.83, 35.04, 31.11. IR (CCl_4): ν 2957, 2924, 2854 cm^{-1}. UV/vis (CH_2Cl_2): λ_{max} (ϵ) 230 (73 900), 300 (60 000), 342 (74 600), 356 (66 000) nm. MS (CI pos) *m/z* (%): 867 (M^+ + THF, 100), 796 (MH^+, 19), 372 (50); $C_{62}H_{50}$ (795.06).

Crystallographic Data. Intensity data for **9** were collected at 293 K and for **10**, **12**, **15**, and **18** at 153 K on a Bruker SMART-APEX diffractometer using Mo Kα radiation (λ = 0.7107 Å). Lorentz and polarization corrections were applied and diffracted data were also corrected for absorption using the SADABS program. Structures were solved by direct methods and Fourier techniques. Structure solution and refinement were based on $|F|^2$. All non-hydrogen atoms were refined with anisotropic displacement parameters except for the carbon, oxygen, and chlorine atoms of the solvent molecules in **9**, **10**, and **18**. In **9**, the THF solvent molecule was highly disordered and solved as a group of five carbon atoms. The H atoms of the C−H groups were fixed in calculated positions. In **15**, three of the six Et-groups attached to the phosphorus atoms were disordered and refined with two equally occupied sets of coordinates. Intensity data for **4** and **8** were collected at 293 K on a Nonius CAD-4 serial diffractometer. In **4** the *tert*-butyl and ethyl moieties were disordered and left isotropic. The *tert*-butyl moiety was observed to be disordered over two positions, and the corresponding carbon atoms were refined with occupancies of 0.5.

Acknowledgment. This research has been supported by the National Science Foundation (CHE-0414175). C.A.J. acknowledges the NSF for an IGERT fellowship. The CCD diffractometer was purchased with funds provided by the NSF (CHE-0234965).

Supporting Information Available: X-ray structures for **4**, **8**−**10**, **12**, **15**, and **18**. This material is available free of charge via the Internet at http://pubs.acs.org.

OM0490987